摩擦焊接轴向缩短量神经网络与支持向量机预测

王非凡[1]， 李文亚[1]， 刘 卫[2]
(1. 西北工业大学 凝固技术国家重点实验室，西安 710072;
2. 青海师范大学 物理系，西宁 810008)


王非凡

摘 要：轴向缩短量是惯性摩擦焊接过程中的关键参量. 文中利用 ABAQUS 有限元软件对高温合金管材惯性摩擦焊接过程进行了模拟，获得并研究了不同焊接工艺参数下的轴向缩短量结果. 基于模拟结果，分别建立了支持向量机(SVM)和径向基函数(RBF)神经网络的轴向缩短量的预测模型. 两种模型的对比表明，对于该小样本的预测，RBF 神经网络比 SVM 智能预测结果更接近有限元模拟值. 因此 RBF 神经网络模型可以更好的辅助摩擦焊接的有限元模拟，并有效降低模拟的时间成本.

关键词：惯性摩擦焊；轴向缩短量；支持向量机；RBF 神经网络
中图分类号：TG404 **文献标识码**：A **文章编号**：0253-360X(2013)03-0085-04

0 序 言

摩擦焊接凭借其优质、高效、节能的工艺特点已被广泛应用于航空、航天及能源等领域. 焊接过程中轴向缩短量是焊接工艺检测的重要参数之一，是焊接构件精密控制的关键技术. 因此研究工艺参数对焊接轴向缩短量影响对于焊接过程及接头质量控制具有重要的指导意义. 数值模拟作为试验研究的一个重要辅助手段，可显著降低试验成本. 然而由于焊接工艺参数的连续变化性，数值模拟的方法亦难以获得任意参数条件下的焊接情况. 因此根据已有试验与模拟结果建立合适的数学预测模型，将具有重要的工程意义.

在熔焊研究中，人工神经网络(artificial neural network，ANN)已被广泛用于焊缝及熔池形貌与力学性能的预测[1]，在摩擦焊接的应用正在逐渐展开. Okuyucu 等人[2]曾采用 BP 算法预测了搅拌摩擦焊接工艺参数对铝板机械性能的影响. Kumaran 和 Sathiya 等人[3,4]则分别将 ANN 用于优化铝合金和不锈钢的摩擦焊接研究. 此外支持向量机(support vector machine，SVM)作为一种较新型的智能数学方法，尚未有摩擦焊应用的研究报道.

文中将采用 Abaqus 模拟软件建立完全热力耦合二维有限元模型，并利用网格重划分技术对高温合金 GH4169 管材的惯性摩擦焊接过程进行计算，分析焊接工艺参数轴向缩短量的影响. 根据模拟结果，分别建立并分析 RBF 神经网络和 SVM 算法的轴向缩短量预测模型. 为摩擦焊接精密控制与工艺参数提供理论依据，并进一步降低研究成本.

1 数值模拟

1.1 数值模型

在前期工作的基础上[5,6]，图 1 为惯性摩擦焊接几何模型与二维轴对称网格模型. 模型采用的 GH4169 高温合金管内径 15 mm，壁厚 4 mm. 网格初始划分采用了梯度网格，并采用了网格重划分及映射技术，在计算求解过程中进行网格自动重划分以消除畸变.

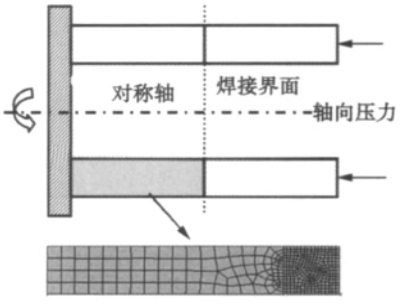

图1 计算模型
Fig. 1 Numerical model

收稿日期：2011-12-07
基金项目：国家自然科学基金资助项目(51005180)；霍英东教育基金资助项目(131052)

焊接过程中飞轮能量转化为焊接热能由子程序根据摩擦耗能计算,可表示为

$$E_{t+\delta_t} = E_t - \omega_t \delta_t \int_S f_s r \mathrm{d}S \tag{1}$$

式中: ω_t 为飞轮瞬时转速; δ_t 为时间增量步长; r 为径向距离; S 为 r 的积分范围. 此外, f_s 表示摩擦力,可分为低温阶段固定值和高温阶段当量值. 高温阶段摩擦行为可视为 Norton-Hoff 剪切层的剪切屈服应力 τ,即

$$\tau = -\alpha p \mu V_t / |V_t| \tag{2}$$

计算给出了 GH4169 高温合金材料随温度变化的热物性参数[7],并运用 Johnson-Cook 材料模型考虑了材料的应变强化、应变速率硬化和温度软化效应[8].

为研究不同焊接工艺条件对焊接轴向缩短量的影响,表 1 给出了模拟研究的工艺参数,其中飞轮转动惯量保持不变. 由于实际惯性摩擦焊接过程很短,计算过程忽略了焊件与环境换热及热辐射的影响.

表 1 惯性摩擦焊接工艺参数

Table 1 IFW processing parameters studied

轴向压力 p/MPa	初始旋转速率 v/(rad·s^{-1})
250, 300, 350, 375, 400, 450, 475, 500	122.8, 132.8, 142.8, 152.8, 162.8

1.2 模拟结果

典型工艺参数初始转速 152.8 rad/s、轴向压力 400 MPa 条件下温度场与轴向缩短量的模拟结果已在作者前期工作[5,6]发表,图 2 所示为不同时刻接头典型形貌及温度分布. 焊接起始阶段接头温度迅速上升但没有飞边形成,此后在 2.5 ~ 4 s 时间段内飞边迅速长大. 随着焊接时间进一步延长,在 4 ~ 4.3 s 时间段内,飞边几乎不变,这是由于摩擦结束阶段工件旋转速度急剧下降,摩擦产热量已不足以挤出飞边. 此外,模拟缩短量 6.2 mm 与试验值[9](约 5.7 mm)接近.

图 3 所示为不同初始转速条件下轴向压力对缩短量的影响. 从图 3 中可以看出缩短量随轴向压力的增大呈指数增长,且在不同的初始转速条件下其变化规律基本相似.

图 4 所示为不同压力条件下初始转速对缩短量的影响,且缩短量几乎随初始转速呈线性增加. 必须指出的是,以上两图可以看出形成缩短量必需满足对应的工艺参数临界条件,为进一步获得各临界参数,作者将采用数学智能预测办法来进行研究.

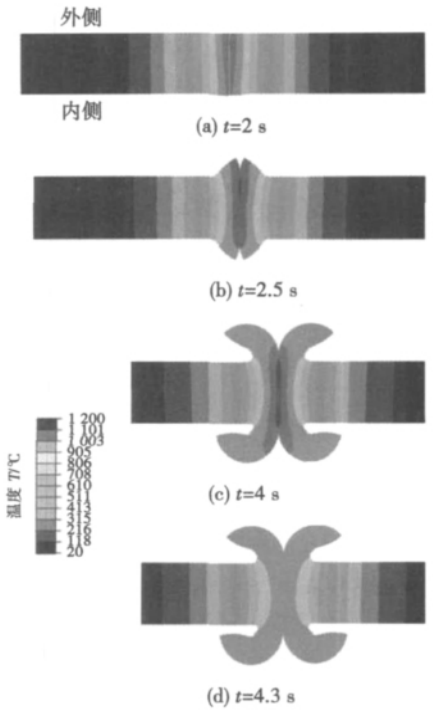

图 2 不同焊接时刻的接头形貌及温度分布

Fig. 2 Variations of joint outline and temperature distribution

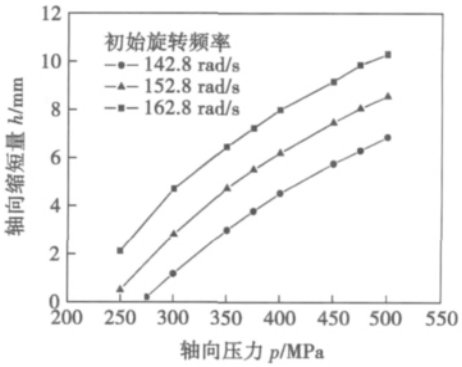

图 3 轴向压力对缩短量的影响

Fig. 3 Effect of axial pressure on total axial shortening

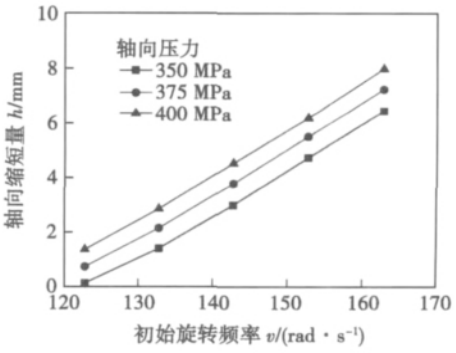

图 4 初始旋转频率对缩短量的影响

Fig. 4 Effect of initial rotational speed on axial shortening

2　数学预测

2.1　SVM 预测结果

SVM 算法作为一种可训练的机器学习方法，常用于建立小样本学习模型以期推广到更高维非线性空间的预测. 根据表 1 所示的工艺参数及相应的模拟结果作为训练样本，分别获得了轴向压力(图 5a) 与初始旋转频率(图 5b) 对缩短量影响的 SVM 预测结果. 通过预测模型将工艺参数与轴向缩短量关系的更宽范围的预测，可更容易获得不同初始旋转频率条件下发生轴向缩短的临界压力值，而不同压力条件下的临界初始旋转频率同样可以较好预测. 然而，对没有参与 SVM 算法训练的一组数据进行了验证对比，结果显示在高旋转频率条件下，SVM 预测与 FE 预测值存在较大偏差.

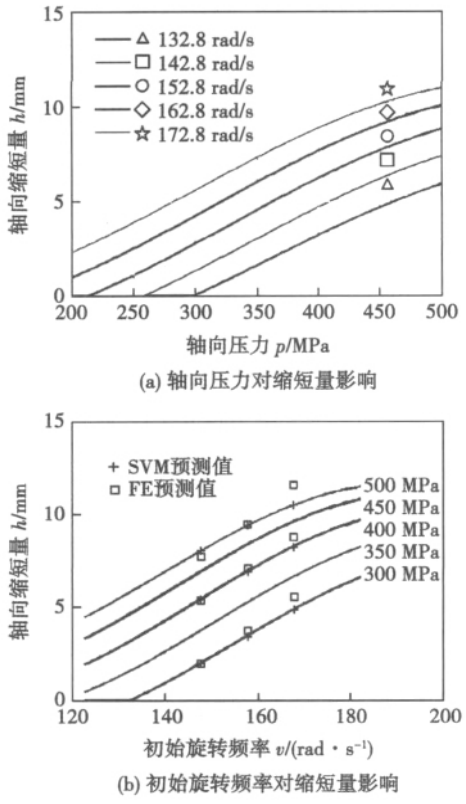

图 5　工艺参数对轴向缩短量影响的 SVM 预测结果

Fig. 5　Effects of parameters on upset predicted by SVM

2.2　RBF 预测结果

RBF 神经网络为单隐层结构的三层前馈网络，是一种局部逼近的网络，它能以任意精度逼近任一连续函数. 根据表 1 工艺参数对应的 FE 模拟结果，最终建立了具有 25 结点中间隐层的 RBF 神经网络预测模型. 图 6 分别给出了 RBF 模型预测的轴向压力与初始旋转频率对轴向缩短量的影响. 图 6 中可以看出，RBF 预测的工艺参数对焊接轴向缩短量影响的预测效果明显优于前面所述 SVM 预测模型.

图 6a 表明不同的初始旋转频率下发生轴向缩短的具有临界压力值，这为摩擦焊接工艺参数选择提供了重要参考. 图 6b 为不同压力下初始旋转频率对轴向缩短量的影响，可以看出缩短量与初始旋转频率呈近线性关系，这与模拟结果(图 4) 非常接近. 同样，通过对没有参加 RBF 神经网络训练的一组数据进行了验证对比可以看出，RBF 预测值与 FE 预测值基本重合. 因此 RBF 预测模型可以更准确地预测工艺参数与轴向缩短量的关系，从而有效地辅助 FE 模拟并减小计算模拟的工作量及时间成本.

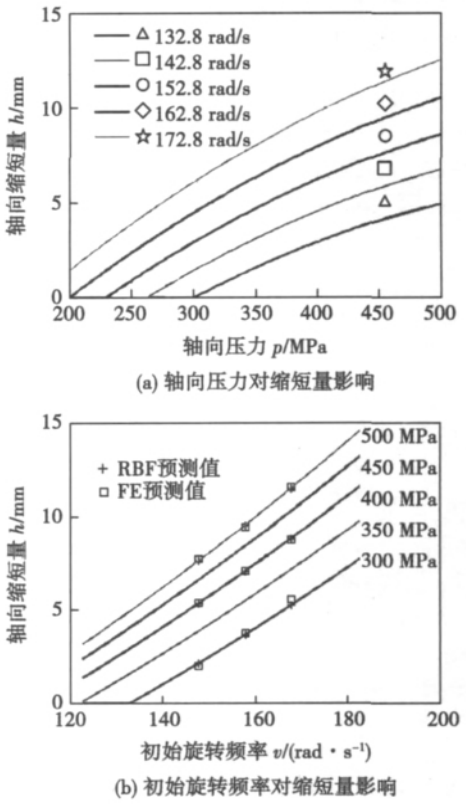

图 6　工艺参数对轴向缩短量影响的 RBF 预测结果

Fig. 6　Effects of parameters on upset predicted by RBF

综合以上讨论与结果分析，在模拟结果的基础上，初步建立了 RBF 和 SVM 惯性摩擦焊接轴向缩短量数学预测模型，而且 RBF 预测效果更佳. 该研究同时也表明了人工数学预测模型在惯性摩擦焊接应用可行，通过建立合理的人工数学智能模型进一步开展惯性摩擦焊接头组织演变和力学性能预测具有重要工程价值.

3 结 论

(1) 建立了惯性摩擦焊接过程完全热力耦合的二维轴对称模型,且模拟结果与试验值吻合较好.

(2) 利用有限元模拟值分别建立了支持向量机和 RBF 神经网络预测模型,且两者均可预测发生轴向缩短的临界工艺参数.

(3) 数学预测与有限元模拟值验证对比发现,RBF 神经网络预测模型可更好地辅助有限元模拟,减小计算模拟的工作量与时间成本.

参考文献:

[1] Benyounis K, Olabi A. Optimization of different welding processes using statistical and numerical approaches-A reference guide [J]. Advances in Engineering Software, 2008, 39: 483 - 496.

[2] Okuyucu H, Kurt A, Arcaklioglu E. Artificial neural network application to the friction stir welding of aluminum plates [J]. Materials and Design, 2007, 28(1): 78 - 84.

[3] Kumaran S, Muthukumaran S, Vinodh S. Optimization of friction welding of tube to tube plate using an external tool by hybrid approach [J]. Journal of Alloys and Compounds, 2011, 509(6): 2758 - 2769.

[4] Sathiya P, Aravindan S, Noorul H A, *et al*. Optimization of friction welding parameters using evolutionary computational techniques [J]. Journal of Materials Processing Technology, 2009, 209(5): 2576 - 2584.

[5] 王非凡, 李文亚, 陈 亮, 等. 轴向压力对惯性摩擦焊的影响数值分析 [J], 焊接学报, 2012, 33(2): 41 - 44.
Wang Feifan, Li Wenya, Chen Liang, *et al*. Numerical study on influence of axial shortening on inertia friction welding [J]. Transactions of the China Welding Institution, 2012, 33(2): 41 - 44.

[6] Chen Liang, Li Wenya, Li Jinglong. Effect of rotation speed on the temperature field and axial shortening of inertia friction welded GH4169 joints by numerical simulation [J]. Journal of Shanghai Jiaotong University (Science), 2011, 16(3): 277 - 280.

[7] 师昌绪, 李恒德, 周 廉. 材料科学与工程手册(上卷) [M]. 北京: 化学工业出版社, 2004.

[8] Demange J J, Prakash V, Pereira J M. Effects of material microstructure on blunt projectile penetration of a nickel-based super alloy [J]. International Journal of Impact Engineering, 2009, 36(8): 1027 - 1043.

[9] 杨 军, 楼松年, 周 昀, 等. GH4169 高温合金惯性摩擦焊接头动态再结晶过程 [J]. 航空材料学报, 2002, 22(2): 8 - 11.
Yang Jun, Lou Songnian, Zhou Yun, *et al*. The dynamic recrystallization properties of superalloy GH4169 inertia friction welding joint [J]. Journal of Aeronautical Materials, 2002, 22(2): 8 - 11.

作者简介: 王非凡,男,1987 年出生,博士. 主要从事摩擦焊接研究工作. 发表论文 9 篇. Email: wangifw@hotmail.com

通讯作者: 李文亚,男,教授. Email: liwy@nwpu.edu.cn

[上接第 84 页]

[4] Jelmorini G, Ticheelaar G W, Essers W G. Wedling characteristics of plasma-MIG process [J]. Metal Construction, 1975, 7(11): 568 - 572.

[5] Jelmorini G, Tichelaar G W, Essers W G, *et al*. Welding characteristics of the Plasma-MIG process [J]. Metal Construction, 1975, 7(1): 568 - 572.

[6] 周大中, 孙 军, 黄子平. 单电源等离子-MIG 焊方法 [J]. 焊接学报, 1990, 11(3): 1 - 3.
Zhou Dazhong, Sun Jun, Huang Ziping. Single power source Plasma-Mig welding process [J]. Transactions of the China Welding Institution, 1990, 11(3): 1 - 3.

[7] Gerardus Jelmorini, Enidhoven. Method of and device for plasma-MIG Welding: U. S Patent, 4146772 [P]. 1979.

[8] Ton H. Physic properties of the plasma-MIG welding arc [J]. Journal of Physics D: Applied Physics, 1975, 8(8): 922 - 933.

[9] 杨春利, 林三宝. 电弧焊技术 [M]. 哈尔滨: 哈尔滨工业大学出版社, 2003.

作者简介: 杨 涛,男,1982 年出生,博士研究生. 主要从事机器人智能焊接及高效焊接方法. 发表论文 10 余篇. Email: 889268@qq.com

joints in the retraction part fractured in the heat-affected-zone (HAZ) on retreating side. The tensile strength and elongation of the bead were 70% and 80% of the base metal, respectively. The retraction speed of stir-pin had remarkable effect on the mechanical properties of the joints, and when the retraction speed was 6 mm/min, the elongation of the joints reached the maximum. The lowest microhardness located in the boundary between TMAZ and HAZ.

Key words: refilling friction stir welding; 2219 aluminum alloy; microstructure; mechanical property; microhardness

Influence of underlaying granular flux with different shapes of metal mesh on formation of ultra-narrow-gap weld
ZHENG Shaoxian, HAN Feng, LI Xiaolei, LI Fanghong (School of Mech-Electronic Technology, Lanzhou Jiaotong University, Lanzhou 730070, China). pp 77 - 80

Abstract: The technology of underlaying granular flux with different shapes of metal meshes has an important influence on the formation of ultra-narrow-gap weld. The ultra-narrow-gap welding was carried out using the technology of underlaying granular flux with three kinds of metal meshes with "V", "U" and "semicircular" structures, respectively. According to the obtained morphology of cross section of ultra-narrow-gap weld, the influence of underlaying granular flux with different shapes of metal meshes on the formation of ultra-narrow-gap weld was analyzed, and then the mechanism of underlaying granular flux with metal mesh preventing arc from discontinuous burning was also clarified. The results indicate that with the increase of surface area covered by granular flux below the sidewalls, the constricting action from melting flux cooling arc could be enhanced and constricting angle of arc α decreased, which led to the decrease of melting height on sidewalls. If melting height was lower than the filled height of melted wire, a convex weld would be produced. Underlaying granular flux with metal mesh could benefit to form cathode spot rapidly on the surface of workpiece and increase the melting of granular flux, which could make the travel speed of cathode zone be equal to that of wire tip along the horizontal direction, consequently, the arc column would not be stretched and the arc could burn continuously and steadily.

Key words: underlaying granular flux with metal mesh; ultra-narrow-gap welding; formation of weld

Plasma-MIG hybrid arc welding with PID increment constant current or voltage control algorithm
YANG Tao[1], ZHANG Shenghu[1], GAO Hongming[1], WU Lin[1], XU Kewang[2], LIU Yongzhen[2] (1. State Key Laboratory of Advanced Welding and Joining, Harbin Institute of Technology, Harbin 150001, China; 2. Offshore Oil Engineering Co. Ltd, Tianjin 300451, China). pp 81 - 84, 88

Abstract: Output characteristics of the power supply and welding process control are important factors for plasma-MIG hybrid arc welding. PID increment control algorithm suitable for Plasma-MIG hybrid arc welding was developed based on VC++ language in this paper, which optimized the output characteristics of the power supply and welding process control. The results show that the plasma arc and MIG arc were coupled with each other by sharing the electro-magnetic space, gas and filler metal. Plasma arc controlled by PID increment control algorithm was capable of stabilizing the current density through the arc due to its self-adjusting function, without sputtering in the welding process. High stability, molten metal with excellent liquidity and weld with smooth surface were realized by plasma-MIG hybrid arc welding with PID increment control algorithm.

Key words: plasma-MIG hybrid arc; PID increment control; welding process control; output characteristic

Prediction of axial shortening in inertia friction welding by RBF and SVM methods
WANG Feifan[1], LI Wenya[1], LIU Wei[2] (1. State Key Laboratory of Solidification Processing, Northwestern Polytechnical University, Xi'an 710072, China; 2. Department of Physics, Qinghai Normal University, Xining 810008, China). pp 85 - 88

Abstract: The accurate control of axial shortening is a key factor for precise inertia friction welding. The inertia friction welding of high-temperature alloy was numerically simulated with ABAQUS finite element (FE) software, and the effects of welding parameters on the axial shortening were investigated. According to the simulated results, two models based on support vector machine (SVM) algorithm and radial basis function (RBF) neural network were developed to predict the axial shortening. By comparing two models, it is found that RBF neural network model showed a better agreement with the FE simulations than the SVM algorithm. Therefore, the RBF neural network could be helpful for FE modeling of inertia friction welding and reducing the time cost.

Key words: inertia friction welding; upset; support vector machine; RBF neural network

Influence of post weld heat treatment on fracture toughness of DH36 steel welded joints
WEN Zhigang[1], JIN Weiliang[1], ZHANG Jianli[1], DENG Caiyan[2] (1. Offshore Oil Engineering (Qingdao) Co. Ltd., Qingdao 266555, China; 2. School of Materials Science, Tianjin University, Tianjin 300072, China). pp 89 - 92

Abstract: Based on the BS7448 standard, the crack tip opening displacement (CTOD) tests were conducted on the weld metal and heat-affected zone (HAZ) of DH36 steel joint, which was made with submerged arc welding (SAW) process and then followed by post weld heat treatment (PWHT), to investigate the influence of PWHT on fracture toughness. The results demonstrate that PWHT did not always produce positive effects on fracture toughness of weld metal. Especially, PWHT had negative influence on fracture toughness of HAZ with coarsened grains, and the CTOD values in coarsened HAZ decreased. After PWHT, the CTOD value of weld metal from 90 mm thick specimen slightly descended, while that from 60 mm thick specimen obviously increased. The CTOD value of HAZ from 90 mm thick specimen descended severely, while that from 60 mm thick specimen descended slightly.

Key words: crack tip opening displacement; submerged arc welding; post weld heat treatment; fracture toughness

Application of ADRC in position servo system for billet flash butt welding
GUO Dong[1,2], FU Yongling[3], LONG Man-